The Total Irradiance Monitor (TIM) for the EOS SORCE Mission

George M. Lawrence*, Gary Rottman, G. Kopp, J. Harder, Wm. McClintock, and T. Woods, University of Colorado, Laboratory for Atmospheric and Space Physics (LASP)
1234 Innovation Dr. Boulder, CO 80303

ABSTRACT

The Total Irradiance Monitor (TIM), to be launched in 2002 on the NASA Earth Observing System (EOS) SOlar Radiation and Climate Experiment (SORCE), will stare at the Sun for five years, and measure the absolute total solar irradiance (TSI). The TIM is an active cavity radiometer with a relative standard uncertainty 100 ppm and a fractional stability of ≤ 10 ppm/year. The estimated uncertainties are "type B" determined from the parametric uncertainties in a model of the instrument; and the dominant uncertainty will be in the effective aperture area. To obtain such low uncertainty, we: 1. Use metallic NiP as the cavity (diffuse) black. 2. Retrieve the irradiance in the frequency domain. 3. Use phase sensitive detection. 4. Use four separate, duty-cycled cavities. 5. Measure the aperture transmission integral over area. 6. Use diamond thermal/electrical nodes. 7. Use 400 seconds for each completely independent data point for low noise. 8. Use a pulse-width-modulated "standard digital watt" as the onboard standard. 9. Take advantage of the 1 ppm noise level to discover systematic effects. 10. Measure IR shutter radiation from in-flight measurements of dark space.

We compare with other TSI measurements on orbit, and as separate shuttle experiments.

Keywords: Radiometry, solar constant, solar irradiance, primary radiometer, accuracy, apertures, lock-in, NiP black, SORCE

1. SOLAR IRRADIANCE MEASUREMENTS

The Total Irradiance Monitor[1] (the TIM, or "TIM") will launch in the summer of 2002 on the NASA Earth Observing System (EOS) SOlar Radiation and Climate Experiment (SORCE)[2], will stare at the Sun for five years, and measure the absolute total solar irradiance (TSI). The TSI, sometimes erroneously called the solar "constant", varies by ±3.6% annually from ellipticity of the Earth's orbit; and when corrected to a standard distance of 1 AU is near 1368 W/m^2. However, there are 27-day variations of several thousand ppm as sunspots rotate with the Sun; and the various flight experiments disagree with each other by a few thousand ppm. Our requirement for TIM is 100 ppm standard relative uncertainty (0.01%, 1 sigma, fractional uncertainty) and a stability of 10 ppm/year in the final measured TSI. The statistical noise level (precision) of TIM is less than 1 ppm.

2. RADIOMETRY

The first measurements of the power flux density of the Sun (solar irradiance) were made through the atmosphere by K. Ångstrom[3] at the end of the 19th century. Ångstrom and, at about the same time, Kurlbaum[4], used an electrical substitution radiometer (ESR) to quantify the radiant power in the beam against the electrical watt. Detailed accounts of ESRs and solar measurements up to about 1987 are given by Hengstberger[5] and by Kmito and Sklyarov[6]. Descriptions of previous space flight missions are given by Willson[7], Willson and Helizon[8], Fröhlich, et al[9,10], and Crommelynck and Dewitte[11].

Before 1982, absolute radiation measurements were generally made with room temperature[5,12,13] ESRs. Circa 1983, it was perceived that the lack of temperature gradients and the much-reduced thermal infrared background in a cryogenic radiometer[14-16] would greatly reduce the systematic uncertainties compared with radiometers working at ≈25°C. However, ambient temperature radiometers, operating with input powers ≥50 mW, rival[5,12,13] cryogenic radiometers. Proposals for a space flight cryogenic radiometer have so far been unsuccessful, presumably because of the high expense, mass, and worries about condensable materials from the spacecraft. TIM will be an ambient temperature radiometer for these reasons. Given the high solar radiance, an ambient temperature radiometer can have sufficiently low noise and uncertainty.

*Correspondence: Email: George.Lawrence@Colorado.edu; Telephone: 303 492 5389 Fax: 303 492 6444

Earth Observing Systems V, edited by William L. Barnes, Proceedings of SPIE Vol. 4135 (SPIE, Bellingham, WA, 2004) · 0277-786X/04/$15 · doi: 10.1117/12.494214

The best radiometric accuracy claimed by the bureaus of standards of the world is about 100 ppm for measurement of ≈1 mW laser beam[15-17] or the measurement of the Stefan-Boltzman constant[18]. Therefore, TIM's requirement of 100 ppm is challenging. The Sun in space, however, is in several ways an ideal measurement source: A. At the Earth, the irradiance is extremely uniform across the aperture of the instrument, simplifying the averaging integrals between instrument sensitivity and source variation. B. The angular distribution of the Sun is a fairly uniform ½° disk at infinity. C. The irradiance is stable, high (≈ 5900K), and predictable in the short term to < 200 ppm. D. The color temperature is ≈ 5900K, putting most of the energy in the visible. Indeed, because of these unique properties, it has proven impossible to accurately simulate the Sun as a radiometric source in the laboratory.

Radiometry experts of the world meet biannually at the NewRad[19] conferences, publish proceedings in the international journal Metrologia, and publish many reference documents to aid newcomers[20-23].

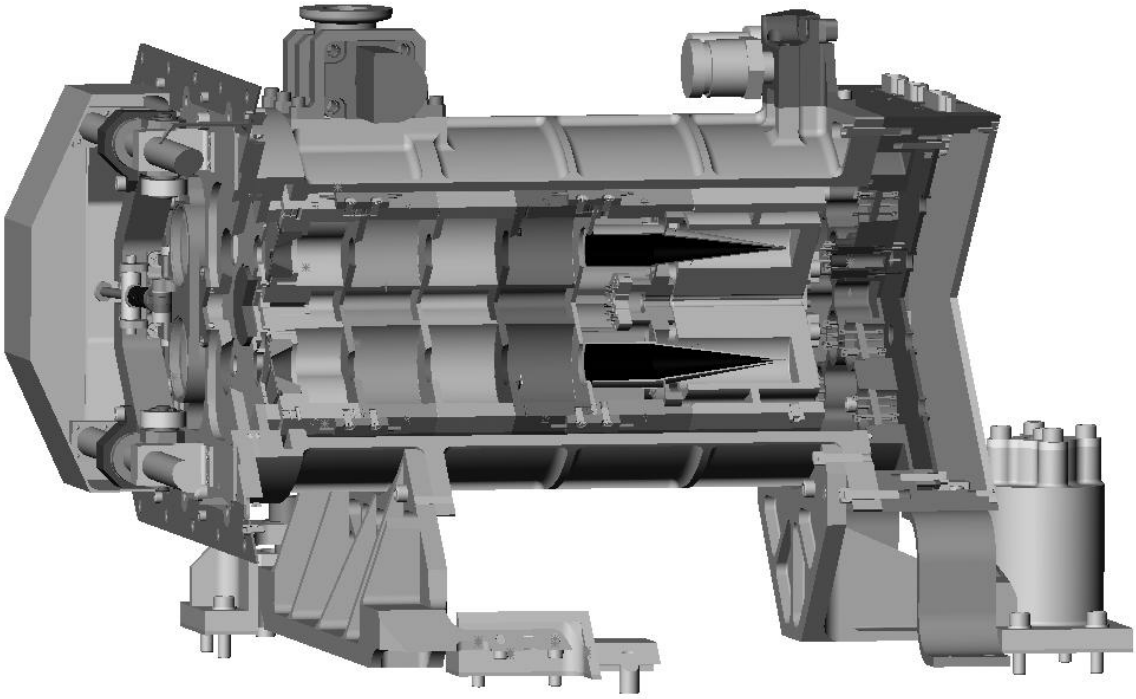

Figure 1 Cut-away of TIM. A vacuum housing with doors maintains cleanliness. Sunlight enters through the shutters and precision apertures at the left, through four baffle sections, and into the black conical cavities. The baffle sections are solid aluminum with no thermally insulating joints. The four cones are supported from a common, cantilevered hub to attenuate thermal signals from thermal gradients. The rear electronics board contains the preamplifiers, two voltage references, pulse-width modulator switches, and housekeeping circuits.

The estimation of the uncertainty (accuracy) of the measurements made by a primary radiometer such as TIM heavily relies on the theoretical analysis of the system, since the measurements themselves depend strongly on a model of the instrument. To estimate uncertainties, we make a high fidelity parameterized model of TIM, invert the model to obtain the "measurement equation", then propagate the parameters and their uncertainties through the measurement equation to the final irradiance. The various uncertainties will add in quadrature, if their distributions have zero mean. We propagate the uncertainties numerically with the parameter spread implemented with pseudo-random numbers. The standard deviation of the parameter-propagated irradiance then gives the system uncertainty estimate. Such uncertainties are named[20,21] "type B" in contrast to empirical statistical uncertainties which are called "type A". The danger, of course, is that some important effect will be omitted from the model. The plan is that sufficient engineering and characterization, supported by the 1 ppm measurements during consistency tests, will reveal the important effects. It would provide closure to verify TIM's absolute accuracy by determining the Stefan-Boltzman

constant[18] or some other physical constant; but such an effort is beyond the scope and budget of the SORCE project.

3. DESIGN OF TIM

TIM, shown in Fig. 1, with parameters summarized in Table 1, is a four-cavity radiometer.

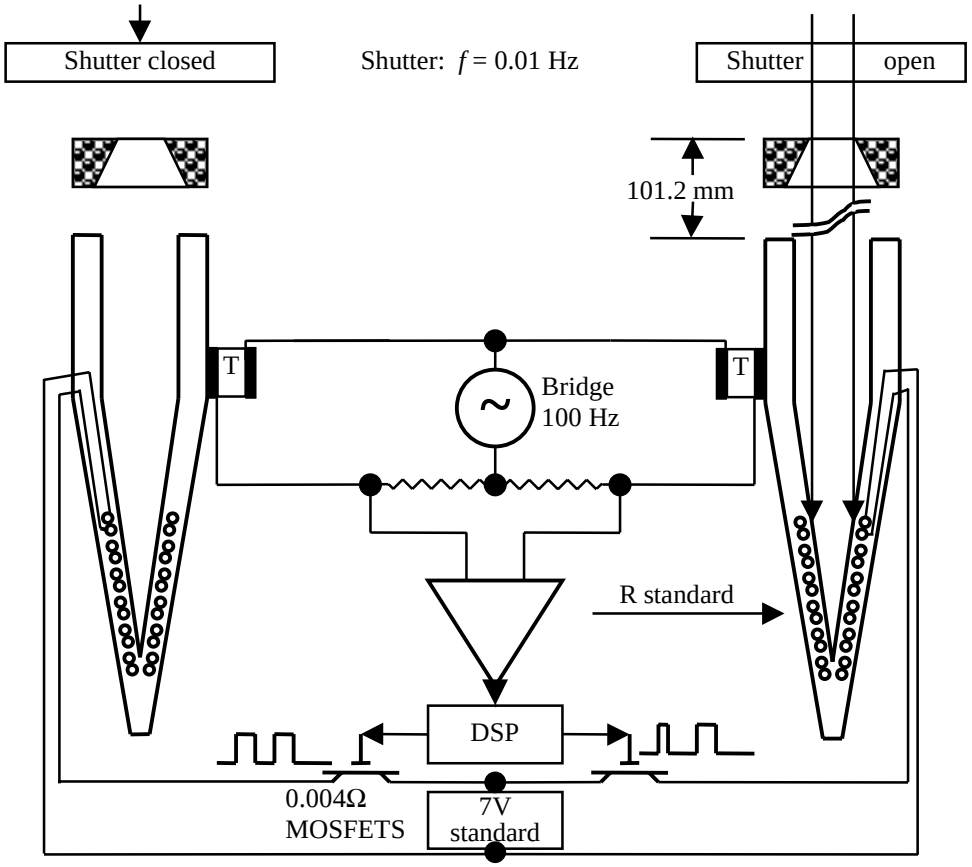

Figure 2 Block diagram of the temperature-balancing bridge for one of the two pairs of cones. Thermistors T at the center of the cones detect temperature changes. The bridge error feeds back through the Digital Signal Processor (DSP) to the replacement heaters embedded in the walls of the cones, maintaining near zero temperature difference. A separate temperature loop, not shown, sets the common mode operating point. The standard voltage is duty-cycled switched by the DSP through low resistance MOSFETs to the wire-wound standard heater resistances, providing the flight standard digital watt. See Fig. 4 for the loop analysis.

A TIM analysis, with a measurement equation, is given in our NewRad99 paper[1]. To measure the solar irradiance (W/m^2), we fly an artifact 100 mW standard (a voltage and a resistance) and an artifact 50 mm^2 standard (a precision aperture). Sunlight entering TIM (Figs. 1 & 2) first encounters a shutter operating at 0.01 Hz, then the precision aperture, a baffle section, and then is absorbed into a thermostatted black, conical silver cavity. An adjacent identical "reference" cavity with the shutter closed provides compensation for temperature changes of the mounting structure. The prototype instrument demonstrates < 1 ppm noise for each 400 sec data point. There are 16 temperature sensors in TIM to provide corrections and analysis of thermal changes.

3.1 Phase Sensitive Detection Algorithm

The raw data from TIM are the various (digital) pulse widths, linear functions of the power changes needed to thermostat the active cone during shutter operation. Traditionally, one would wait for some dead time after shutter operation for the system to stabilize and then average a portion of the power data, subtracting from a similar average for the other half shutter cycle. The concept was to make measurements only at the

eventual stabilization point. TIM's new algorithm uses all of the digital data vs time during the cycle and makes a weighted average with sines and cosines at the shutter fundamental frequency. This is called the lock-in or phase sensitive detection method. The lock-in technique became a ubiquitous part of laboratory detection with the commercialization of Robert Dicke's lock-in amplifier[24]. Usually, however, the goal of lock-in detection is to extract a weak periodic signal from random noise. Here, the goal is to accurately quantify the amplitude of the fundamental in phase with the signal. In the usual laboratory chopping of a light beam, the chopping waveform is poorly known, making it difficult to analyze the beam intensity in the frequency domain. However, with TIM's 0.01 Hz shutter, the shutter waveform component at the fundamental is known to better than 1 ppm.

Harold Black invented and patented[25] electronic negative feedback to reduce distortion (non-linearity) in telephone circuits, analyzing in the frequency domain. Since then, the theory of digital processing (Z-transforms) has been added and the process greatly sophisticated[26-29]. Still, however, the emphasis has been on keeping the system stable and reducing distortion rather that quantifying the signal amplitudes. For example, Clare and White's analyses[30,31] (in the frequency domain) of radiometer servo systems concentrated on settling properties so that the time domain algorithm could be applied. Our departure is to use the standard frequency-domain analysis at "all" frequencies to stabilize the loop; but to use a more complete frequency domain analysis at the (one) shutter frequency to quantify the irradiance.

Phase sensitive detection in our case involves shuttering of the signal at 0.01 Hz, processing through a linear system, and eventual (on the ground) Fourier-transforming of the signal to get the 0.01 Hz component. The advantages over time domain detection that apply to radiometry include: A. We obtain improved signal/noise ratio compared to time domain analysis. In a thermal system, the higher harmonics are small and do not carry much information content; but do carry excess noise. B. In the frequency domain, time-convolutions become multiplications, greatly simplifying the description of the system. The slow diffusion of heat is very difficult to analyze in the time domain. At the fundamental frequency, however, the transfer of heat can be represented by one complex number, the thermal transfer impedance. The complexity of the analysis is then comparable to a steady state problem, contrasted to a time-dependent problem. C. Many of the uncertainties in the system parameters such as shutter delay, the thermal mass of the cones, or the IR emission of the baffles, cause uncertainties mostly in the out-of-phase component of irradiance so are rejected in the final answer. We "lock" the analysis to the proper phase.

Table 1 TIM Parameters

Parameter	Value
Wavelength Range	"all", slight decrease in absorption in far IR
Relative Standard Uncertainty	100 PPM (1 σ)
Relative Stability	10 PPM per year
Precision	<1 PPM
Size, cm (instrument)	34.7 long x 30.3 wide x 20.7 high
Size, cm (electronics)	26.2 long x 21.8 wide x 6.1 high
Mass	6.634 kg instrument, 2.8 kg electronics
Power	14 W
Design Lifetime	5 yrs
FOV	±2° "uniform" ±6° to geometric cut-off
Pointing Requirement	±10 arcmin for ±10 ppm change
Precision Aperture Size	50 mm^2
Shutter Frequency	0.01 Hz
Time response	4 cycle average, quasi-Gaussian, σ = 57 seconds
Cone Reflectivity (1−α)	100 ppm typical, ≈ 10% uncertainty
Operating Temperature	-15 to 23°C

3.2 Apertures

At a distance of 101.6 mm in front of the four cavities, are four apertures, defining the standard areas of TIM. The apertures are diamond turned from aluminum, with a nominal area of 50 mm^2 and a diameter 7.9788 mm. Aluminum is not the best material for "perfect" edges as the edges have pull-outs and burrs on the order of ½ to 1 μm. However, the aluminum oxide layer gives some protection to the space environment. The area will change +46 ppm/°C so we telemeter aperture temperatures accurate with respect to calibration temperature to 0.1°C.

Previous solar radiometers have put the aperture close to the cavities, with a field of view aperture about 100 mm out front. We have reversed this order, reducing the shuttered stray radiation inside the radiometer, but at the expense of 432 ppm of diffraction correction[32] to the nominal aperture "area". The $zero^{th}$ order concept is that the aperture "area" multiplies the incoming irradiance to produce the power. Due to diffraction and scattering from the edges, however, the simple area concept does not suffice. Granted, the transmission of the aperture through the center is unity; but at the edges, the effective transmission can vary above one and then drop off to zero outside the edge. This effective transmission map depends on the wavelength and the size of the down stream detector. Therefore, we map the transmission from aperture to detector vs wavelength; and then integrate over area to define the transmission integral. With a 16-bit CCD camera, we image the aperture, illuminated with a ½° artificial Sun, and the integrate the normalized transmission over the image. The geometric scale comes from images of an interfereometrically generated Ronchi ruling. Our uncertainty budget is <78 ppm in the effective area integral.

As an independent check of our aperture method, we have procured three calibrated copper apertures from the National Institute of Standard and Technology (NIST). We will theoretically correct their calibration value, a "geometric" area, for diffraction; and compare the corrected values with our measurements.

3.3 Cavity Absorption

Down-stream from the apertures, the conical cavities (mouth diameter 15.6 mm) absorb the 8 mm input beam and all but 432 ppm of the diffracted energy[32], less some reflected energy. We have constructed the cones from electrodeposited silver with an interior coating of NiP black[33,34], also called NBS black. Being a metallic black, it should be more stable than the black paints used in previous space flight radiometers. With laser beam reflectance tests, we find that the cavities reflect ≥50 ppm of the incoming light, averaged over the incoming beam. With a typical cavity reflectance of 100±20 ppm, the cavity absorption is not a large contributor to TIM's system uncertainty.

We have empirically learned that ultrasonic cleaning can degrade the black surface, and NiP, etched too deeply, is fragile to mechanical and thermal shock. We have irradiated a sample in the Synchrotron Ultraviolet Radiation Facility (SURF) at NIST to a level of 4 Coulombs of beam charge (2 weeks exposure). There was a barely visible graying with an estimated surface reflectance change from ≈ 0.9% to ≈ 1%. Unfortunately, we do not have yet a theory to relate SURF damage to solar damage. The SURF beam, however, will destroy the transmission of a fused silica window in about 2 hours, whereas sunlight in space for years hardly affects the transmission[35] except for surface contaminants. Given our uncertainty about the stability of the cavity black, we will duty-cycle the four cavities, in flight, to characterize degradation. There is also a small silicon photodiode viewing each cavity from inside the last baffle section, to detect changes in the reflectance of each cavity. These photodiodes are also useful for normalizing time fluctuations of the solar simulators during tests.

3.4 Standard Watt

As indicated in Fig. 2, the basic digital to analog converter is the pulse-width modulated switching of the standard voltage onto the standard resistors. This gives a heating power having changes linear in the digital pulse width. Thus, all signals in the control loop are linear analogs of the system power changes. The two standard voltage sources use the LTZ1000A[36] buried Zener diode. The sources operate at about 7.1 V with a stability better than 2 ppm/year[37,38], to be tracked against ground witnesses. With an emitter follower output driver and careful attention to single point voltage connections, these voltage sources are able to supply the 13 ma pulse current to the replacement heaters with less than 10 ppm droop and ripple on the waveform.

The standard flight resistors are wire-wound into spiral grooves over a region at the back of the cones, approximating the distribution of absorbed radiation. The polyimide-insulated wire is then vacuum-encapsulated with epoxy and jacketed with 0.125mm of gold-plated copper. The outer gold coating prevents radiative losses, and no heat escapes the wires without flowing through the metallic cone structure. Wound with MWS800[39] wire, these resistors (≈540 Ω) show a temperature coefficient of resistance (TCR) of +15 ppm/°C and a stability better than 5 ppm against months of time and temperature cycles of ±50°C. The copper leads between the MOSFET switch and the heater constitute a ≈125±5 ppm correction to the resistance. The copper leads between the cone and the radiometer are insulated at the ends with soldered, metalized, CVD diamond chips to provide geometric definition for the TIM thermal model.

3.5 Equivalence of Electrical and Radiative Power

Understanding the equivalence between radiative and electrical substitution power requires analysis, vs frequency, of the thermal heat flow in the cone. The word frequency, here implies sinusoidal variation. Given a complex amplitude $\boldsymbol{P}$ for the power applied to the heater, we can express the (complex) temperature amplitude $\boldsymbol{T}$ at the cavity thermistor with a (complex) thermal transfer impedance* $\boldsymbol{Z_h}$ having units of °C/W. $\boldsymbol{T} = \boldsymbol{Z_h}\,\boldsymbol{P}$. The thermal impedance depends upon the thermal properties of the cone and upon the distribution of applied heat. Similarly we can define a radiative thermal transfer impedance $\boldsymbol{Z_r}$ between the absorbed radiative power and the thermistor temperature variations. The relative sensitivity in the measurement equation requires knowledge of the (complex) "equivalence ratio" $\boldsymbol{Z_r}/\boldsymbol{Z_h}$ as derived in §3.6. The equivalence ratio is a factor in the measurement equation for the irradiance conversion.

The equivalence ratio is nearly unity because we have put the region of absorbed radiation (and the heaters) some distance from the thermistors and have gold plated the exterior of the cones. The heat flow from cone tip to thermistor "forgets" the details of the absorbed distributions, except for some phase delay. The phase delay does limit the servo gain somewhat, but only introduces appreciable uncertainty in the out-of-phase (imaginary) part of the equivalence ratio.

We must theoretically determine the equivalence ratio, using empirical values of the model parameters. This is the meaning of a primary radiometer. The ratio could only be measured against a known irradiance source, which does not exist at the 100 ppm uncertainty level. Our plan, however, is to calculate the ratio at zero frequency, then measure the ratio vs shutter fundamental up to the operating point of 0.01Hz. Fig. 3 shows an initial model calculation showing that the eventual uncertainties in the real (in-phase) component of the equivalence ratio will be on the order of 10 ppm.

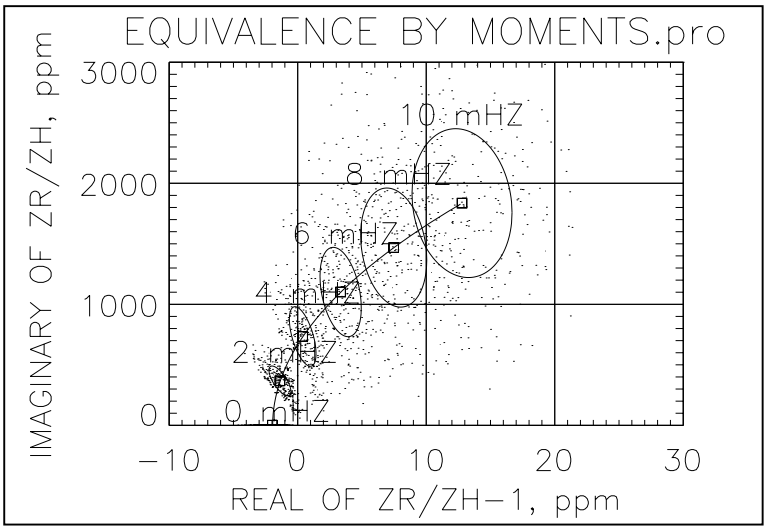

Figure 3 Monte Carlo calculation of the real and imaginary TIM non-equivalence vs shutter fundamental frequency. We calculate, ab-initio, the equivalence at zero frequency, but measure the path to 10 mHz. The parameters and their scatter are plausible, though not yet final. Only the real part affects the irradiance determination. The ellipses at each frequency show one standard deviation.

*Circa 1893, Arthur Edwin Kennelly's paper "Impedance" allowed electrical engineers to use complex numbers in analyzing AC circuits. We apply this concept to alternating thermal flow.

3.6 Servo[#] System

As indicated in Fig. 2, the temperature of the active cone is continuously regulated while the pulse width, and hence power, to the reference cone is kept constant. The active control loop on the right of Fig. 2 contains a digital loop filter operating at a cadence of 100 Hz so there are 10,000 digital data points per shutter cycle. The 10,000 16-bit values of the pulse width form the data stream ***Out*** which monitors power changes into the radiometer.

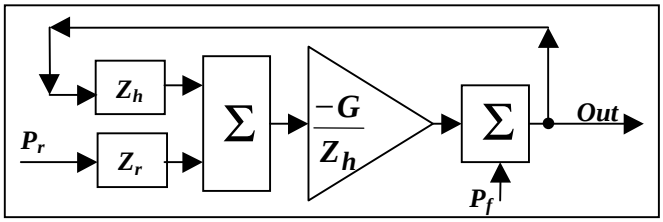

Figure 4 Servo diagram. ***Out*** is the complex response to input radiant power P_r and the feedforward power P_f. Loop gain is G. The left summation node is the thermistor, and the right summation is digital addition in the DSP. The thermal impedances are in °C/W. Signals are in Watts.

Fig. 4 defines the transfer functions and the loop equations for the servo system. At the output there is provision for adding a digital "feed forward" square wave P_f as a test pulser; or to anticipate the power change upon shutter operation. Solving the implicit equation of Fig. 4 for the input radiative power P_r gives:

$$P_r = -\frac{Z_r}{Z_h}\left(Out + \frac{Out - P_f}{G} \right) \qquad (1)$$

Equation (1) relates allows us to measure the input power for any feedforward signal. We see that it is necessary to know the equivalence ratio as discussed in §3.5 and to know the loop gain G. In flight, the gain will be periodically measured by closing the shutters, pulsing the feed forward pulser and solving (1) for G. We also notice from (1) that if we set P_f within, say, 1% of ***Out***, the gain-dependent term will be reduced by a factor of 100. That is, we will apply the feedforward signal based on our expectation of the power signal, and then the servo system will have much less to do. The feed forward matching is thus a way to increase the effective loop gain and hence stability, given a fairly constant source.

The loop filter of the servo is a standard Proportional Integral Difference (PID) filter optimized by the Ziegler-Nichols method[26]. The optimization criteria for the loop filter are that the loop be stable and there be < 10% overshoot so as to not unduly reduce the dynamic range of the system. Exact tuning of the loop gain therefore is not critical. What must be known to a few hundred ppm is the (complex) loop gain G at the shutter fundamental; and this gain is measured periodically in flight by a special DSP program.

4. TIM FLIGHT PLANS

TIM is one of the four science instruments on SORCE, which will be launched into a 600 km Earth orbit from a Pegasus XL in July 2002. The mission has a lifetime of 5 years with a goal of 6 years. Operations are controlled from CU/LASP's Mission Operations Center in Boulder, Colorado. Normal operations and data acquisition begin following a scheduled month of spacecraft outgassing (during which time TIM's vacuum doors remain sealed) and instrument checkout.

4.1 Normal Operations

Operational flexibility, redundancy, and calibration corrections are provided by having four identical cones, A, B, C, & D. The four TIM cones are configured in pairs by the bridge connections (Fig. 2), but each has its own independent shutter. Any of the cone shutters can be controlled at any time, and the active cone can be selected or changed on-orbit.

Normal operations for TIM are continual observations of the Sun during the daytime side of each orbit when the instrument is not pointed within 15° of the spacecraft velocity vector. One cone, A, is the primary active cone, and its shutter operates at 0.01 Hz. This cone is thermally referenced to cone D. As all cones are in nearly identical thermal environments, reference cones compensate for thermal drifts and

[#] Servo: Latin, to follow.

noise in the active cone. Cones B and C, each with a closed shutter, and thermistors on the heat sink provide further diagnostic information on thermal gradients within the instrument cavity. Replacement heater data on each pair of cones are acquired at 100 Hz and stored on-board for subsequent downlink.

4.2 In-flight Calibrations

During the daytime side of the orbit, the active cone alternately views the incident power from the Sun and from its closed shutter, which emits or reflects blackbody radiation characteristic of the instrument temperature. This ≈1800 ppm offset is corrected by measurements of dark space during the nighttime side of the orbit. After passing into the Earth's shadow, the spacecraft slews to observe calibration stars for another on-board instrument. During these observations, shutter-modulated measurements with TIM provide knowledge of the amount of shutter radiation detected by the active cone. Together with measurements of the shutter's temperature provided by the thermistor embedded in each shutter, this allows for a correction accounting for the modulated shutter signal during solar observations.

A weekly cruiciform alignment maneuver allows for calibrations of alignment offsets between the SORCE instruments and the Sun sensors, and corrects for gains in the Sun sensors. These planned maneuvers are ±4° scans centered on the Sun in orthogonal directions at slew rates of 0.1°/min.

A field of view (FOV) map made periodically on orbit tracks changes in instrument sensitivity as a function of pointing. The 5x5 grid of positions, spaced by 15 arc minutes, will take approximately 15 orbits each 6 months.

Degradation of cone sensitivity from exposure to the Sun is accounted for by duty-cycling the cones. Cone A is nominally the active cone, and receives a significant amount of potentially damaging solar radiation. From simultaneous measurements early in the mission using the cone pairs A&B and A&C, the relative sensitivities of these cones are obtained before any have degraded significantly. Infrequent use of cones B and C during the mission keeps them in a relatively pristine state. We will duty cycle cone B at a 1% rate (i.e. using it for 1 orbit every week) and cone C at a 0.1% rate. Changes in sensitivity of cone A that are seen to a lesser extent in cone B and an even lesser extent in cone C may be attributed to solar exposure degradations. The comparisons between the three cones will thus provide long-term degradation calibration corrections for cone A. Faster comparison cadences early in the mission may account for rapid, short-term solar degradation.

Cone D is used as a thermal reference to cone A and as a redundant backup cone. A relative sensitivity calibration of cone D will be made early in the mission.

In-flight electronic tests include temperature sensor cross comparisons, servo gain measurement, and low frequency shutter operation to measure the frequency dependence of the equivalence ratio.

4.3 Data Analysis and Archiving

The downlink replacement heater data indicate the amount of solar power falling of the active cone. These data are boxcar averaged four times to remove sensitivity to the TIM shutter frequency; giving an independent solar irradiance measurement every 400 sec. This filtering and averaging effectively provides the Fourier component in phase with and at the shutter frequency.

All data are analyzed at CU/LASP. The science data system will produce two TSI data products for each calendar day, including a daily irradiance average and a 6-hour average. LASP will maintain a complete archive of primitive (irreplaceable) data, including telemetry, software and database configuration, calibration data, and job control parameters. Multiple archives will be kept in separate physical locations on a quasi-permanent medium.

Provisional standard data products (unvalidated and using preliminary time-dependent corrections) are distributed to public users within 48 hours of reception via the SORCE web page. The NASA/Goddard Space Flight Center's Distributed Active Archive Centers (DAAC) will receive a completely calibrated data set following the application of empirically-determined time-dependent corrections. As some of the calibration data for these corrections are taken much later than current data, the corrected DAAC data will have approximately a 3 month lag. Updates to the DAAC are planned to occur monthly, and each release will supercede all previous data files.

4.4 Instrument Comparisons

TIM's operational flexibility allows for intra-instrument cone comparisons as well as more traditional inter-instrument comparisons. Three TIM units are being built: SORCE/TIM will fly on the spacecraft; Hitchhiker/TIM will be a mobile unit to facilitate comparisons to other instruments, particularly from NASA's shuttle; and a witness unit will be maintained in a clean environment for future lab measurements. All three TIM instruments are being built and calibrated together, so comparisons between them should be straightforward.

Using two active cones on the SORCE/TIM, each with its own reference cone, provides the capability to obtain simultaneous solar measurements. Thus intra-instrument comparisons between two cones are not affected by short-term solar fluctuations. Early in the mission, each cone will be compared with at least one other cone using simultaneous measurements. This establishes a baseline in cone sensitivity and checks the ground-based characterization of each cone, providing a relative measure of apertures, reflectivities, and thermal sensitivities.

Inter-instrument comparisons are planned between SORCE/TIM and both on-orbit and shuttle-platform radiometers. ACRIMSat's ACRIM III should still be operational after SORCE launch, and ACRIM II may still be acquiring data, allowing direct comparison to TIM and a link to the long-time irradiance record given by these radiometers. SOHO's L1 orbit allows uninterrupted solar monitoring, including irradiance data from VIRGO's DIARAD and PMO6, and these radiometers will likely overlap with the TIM data record.

STS Research Mission 2 will fly shuttle hitchhikers TIM and SOLCON (a near-clone of DIARAD) mounted side-by-side on the same platform to give the most direct comparison between these two instruments. Future shuttle missions will provide comparisons between the SORCE/TIM and the Hitchhiker/TIM, establishing a link between the SORCE measurements and a ground-accessible TIM and providing further means of detecting and correcting for degradations to the SORCE/TIM.

REFERENCES

1. G.M. Lawrence, G.J. Rottman, J.W. Harder, and T.N. Woods, "The solar Total Irradiance Monitor: TIM", *Metrologia,* in press, 2000.
2. T. N. Woods, G. J. Rottman, J. W. Harder, G. M. Lawrence, and B. McClintock, paper 4135-21, this session, *Earth Observing Systems V Proc. SPIE*, **4135**, 2000. See also papers **4135**-22 and **4135**-24.
3. K. Ångstrom, "The absolute determination of the radiation of heat with the electrical compensation pyroheliometer, with examples of the application of this instrument", *Astro-physics*, **9**, 332,1899.
4. F. Kurlbaum, "Über eine Methode zu Bestimmung der Strahlung in absolutem Maass und die Strahlung des schwarzen Körpers zwischen 0 und 100 Grad.", *Wied. Ann.*, **65,** 746, 1898.
5. F. Hengstberger, Absolute Radiometry, Electrically Calibrated Thermal Detectors of Optical Radiation, Academic Press, 1989.
6. A.A. Kmito and Yu.A. Sklyarov, *Pyroheliometry*, Gidrometeoizdat Publishers, Leningrad, 1981, Translated as NBS 0020, 1987 Oxonian Press Pvt. Ltd., New Delhi, also NTIS, 1987.
7. R. C. Willson, "Total Solar Irradiance Trend During Solar Cycles 21 and 22", *Science*, **277**, pp1963-1965, 1997.
8. R.C. Willson, and R. S. Helizon, "EOS/ACRIM III instrumentation" *Proc. of SPIE Earth Observing Systems IV*, **3750**, 233-242, 1999.
9. C. Fröhlich, B. N. Andersen, T. Appourchaux, G. Berthomieu, D. A. Crommelynck, V. Domingo, A. Fichot, M.F. Finsterle, M. F. Gómez, D. Gough, A. Jiménez, T. Leifsen, M. Lombaerts, J. M. Pap, J. Provost, T. Roca Cortés, J. Romero, H. Roth., T. Sekii, U. TellJohann, T. Toutain, and C. Wehrli, In *The First Results from SOHO* Edited by B. Fleck and Z. Svestka, Dordrect /Boston /London, Kluwer Academic Publishers, 1997.pp 1-25. See also *Solar Physics*, **170** and **175**, 1997
10. C. Fröhlich, D.A. Crommelynck, C. Wehrli, M. Anklin, S. Dewitte, A. Fichot, W. Finsterle, A. Jiméniz A. Chevalier, H. Roth, In *The First Results from SOHO* Edited by B. Fleck and Z. Svestka, Dordrect /Boston /London, Kluwer Academic Publishers, pp267-286, 1997. See also *Solar Physics*, , **170** and **175,** 1997.
11. D.A. Crommelynck and S. Dewitte, "Metrology of Total Solar Irradiance Monitoring", *Adv. Space Res.*, **24**, pp195-204, 1999.

12. K. Gibb, J.E. Decker, L.P. Boivin, S.R. Das, and M.A. Buchanan, “Development of improved electrical-substitution radiometers at the National Research Council of Canada”, *Applied Optics,* **35,** pp3607-3613, 1996.
13. M. Simionescu, F. Ionescu, “Real time electric substitution in radiometry”, *Photodetectors and Power Meters II Proc. SPIE,* **2550,** pp91-98, 1995.
14. J.E. Martin, N.P. Fox and P.J. Keys, "A cryogenic radiometer of absolute radiometric measurements," *Metrologia*, **21**, 147 (1985).
15. R.U. Datla, K. Stock, A.C. Parr, C.C. Hoyt, P.J. Miller, and P.V. Foukal, “Characterization of an absolute cryogenic radiometer as a standard detector for radiant-power measurements”, *Applied Optics*, **31,** pp7219-7225, 1992.
16. T.R. Gentile, J.M. Houston, J.E. Hardis, C.L. Cromer, and A.C. Parr, “National Institute of Standards and Technology high-accuracy cryogenic radiometer”, *Applied Optics*, **35,** pp1056-1068, 1996.
17. T.C. Larason, S.S. Bruce, and C.L. Cromer, “The NIST High Accuracy Scale for Absolute Spectral Response from 406 nm to 920 nm”, *J. Research of the National Institute of Standards and Technology*, **101**, pp133-140, 1996.
18. T.J. Quinn and J.E. Martin, "A radiometric determination of the Stefan-Boltzmann constant and thermodynamic temperatures between -408ºC and +1008º C," *Phil. Trans. Roy. Soc. London*, **A316**, p85,1985.
19. *NewRad99 Madrid*, http://newrad.metrologia.csic.es
20. “The NIST Reference on Constants, Units, and Uncertainty”, http://www.physics.nist.gov/cuu/Uncertainty/index.html
21. C.L. Wyatt, V. Privalsky, and R.U. Datla, Recommended Practice; Symbols, Terms, Units and Uncertainty analysis for Radiometric Sensor Calibration, NIST Handbook 152, U.S. Government Printing Office, Washington, 1998.
22. Fluke Corp., Calibration: Philosophy in Practice, 2nd edition, Fluke Corporation, Everett, WA, 1994.
23. *TN 1421* http://physics.nist.gov/Pubs/TN1421/electrical.html NIST web site on ESRs, HACR, Quinn, etc. Paradigm is DC conductance and Infrared losses.
24. W. Happer, P.J.E. Peebles, and D.T. Wilkinson, “Robert Henry Dicke” *National Academy of Sciences, Biographical Memoirs **77***, pp 78-95,1999. http://bob.nap.edu/readingroom/books/biomems/rdicke.html
25. Harold S. Black, “Wave Translation System” (negative feedback) U.S. Patent 2,102,671, 1937.
26. F. Nekoogar, and G. Moriarty *Digital Control using Digital Signal Processing*, pp 246-248, Prentice Hall, 1999.
27. Z. Z. Karu**,** *Signals and Systems Made Ridiculously Simple*, http://zizipress.home.mindspring.com, 1994.
28. R. D. Strum and D. E. Kirk, *Contemporary Linear Systems using MATLAB,* PWS publishing, 1994.
29. B.P. Lathi**,** *Signal Processing and Linear Systems*, Berkeley-Cambridge Press, 1997.
30. J F Clare and D R White. “Optimal design of electrical substitution radiometers with feedback control”, *Metrologia*; **28**, pp. 179-182, 1991.
31. J F Clare and D R White. 1989. “Response time and noise power gain of electrical substitution radiometers with feedback control”, *Applied Optics*; vol. **28**, pp3417-3424, 1981.
32. W. R. Blevin, “Diffraction Losses in Radiometry and Photometry”, *Metrologia*, 6, pp39-44, 1970.
33. C. E. Johnson, “Ultra-black coating due to surface morphology”, U.S. Patent #4,233,107, 1980.
34. C. E. Johnson, “Black electroless nickel surface morphologies with extremely high light absorption capacity”, *Metal Finishing*, pp21-24, 1980.
35. K. Havey, W. Arthur, and J.F. Vallimont, “Effects of long-term space environment exposure on optical substrates and coatings”, in *Damage to Space Optics, and Properties and Characteristics of Optical Glass*, *SPIE Proc*. **1761**, 1993.
36. Linear Technology Corp., Milpitas, CA, www.linear.com
37. P. J. Spreadbury, “The Ultra-Zener—a portable replacement for the Westen cell?”, *IEEE Trans. Instrumentation and Measurement*, **40**, pp343-346, 1991.
38. B.G. Rax, C. I. Lee, and A. H. Johnston, “Degradation of precision reference devices in space environments”, *IEEE Trans. Nuclear Science*, **44**, pp1939-1944, 1997.
39. MWS Wire Industries, Westlake Village, CA